

M. Groth, P. Belo, S. Brezinsek, M. Brix, J.W. Coenen, C. Corrigan, J. Flangan,
D. Harting, A. Huber, S. Jachmich, A. Järvinen, U. Kruezi, M. Lehnen,
C. Lowry, A.G. Meigs, S. Marsen, S. Munaretto, M.F. Stamp
and JET EFDA contributors

Divertor Plasma and Neutral Conditions in JET-ILW Ohmic Plasmas in Semi-Horizontal and Vertical Divertor Configurations

Divertor Plasma and Neutral Conditions in JET-ILW Ohmic Plasmas in Semi-Horizontal and Vertical Divertor Configurations

M. Groth¹, P. Belo², S. Brezinsek³, M. Brix⁴, J.W. Coenen³, C. Corrigan⁴,
J. Flanagan⁴, D. Harting³, A. Huber³, S. Jachmich⁵, A. Järvinen¹, U. Kruezi³,
M. Lehnen³, C. Lowry⁶, A.G. Meigs⁴, S. Marsen⁷, S. Munaretto⁸, M.F. Stamp⁴
and JET EFDA contributors*

JET-EFDA, Culham Science Centre, OX14 3DB, Abingdon, UK

¹ Aalto University, Association EURATOM-Tekes, Otakaari 4, 02150 Espoo, Finland

² Institute of Plasmas and Nuclear Fusion, Association EURATOM-IST, Lisbon, Portugal

³ Forschungszentrum Jülich GmbH, EURATOM-Association, TEC, Jülich, Germany

⁴ EURATOM-CCFE Fusion Association, Culham Science Centre, OX14 3DB, Abingdon, OXON, UK

⁵ Association "EURATOM Belgium State", Lab. for Plasma Physics, Brussels, Belgium

⁶ EFDA Close Support Unit, Culham Science Centre, OX14 3DB, Abingdon, OXON, UK

⁷ Max-Planck-Institute for Plasma Physics, EURATOM Association, Greifswald, Germany

⁸ Consorzio RFX, Association EURATOM-ENEA, Padua, Italy

* See annex of F. Romanelli et al, "Overview of JET Results",
(24th IAEA Fusion Energy Conference, San Diego, USA (2012)).

Preprint of Paper to be submitted for publication in Proceedings of the
40th EPS Conference on Plasma Physics, Espoo, Finland.

1st July 2013 – 5th July 2013

“This document is intended for publication in the open literature. It is made available on the understanding that it may not be further circulated and extracts or references may not be published prior to publication of the original when applicable, or without the consent of the Publications Officer, EFDA, Culham Science Centre, Abingdon, Oxon, OX14 3DB, UK.”

“Enquiries about Copyright and reproduction should be addressed to the Publications Officer, EFDA, Culham Science Centre, Abingdon, Oxon, OX14 3DB, UK.”

The contents of this preprint and all other JET EFDA Preprints and Conference Papers are available to view online free at www.iop.org/Jet. This site has full search facilities and e-mail alert options. The diagrams contained within the PDFs on this site are hyperlinked from the year 1996 onwards.

1. INTRODUCTION

The spatial distribution of deuterium neutrals in the divertor chamber of tokamaks and their dynamics play a key role in achieving detached divertor conditions, the mode of operation foreseen in ITER [1], and in enabling particle (density) control via pumping. In present tokamaks, neutrals due to recycling of plasma ions at plasma-facing components are also one of the main sources of particles in the core plasma, and thus considered to impact the pedestal density [2] and to lead to power losses in the core due to charge exchange with plasma ions. The physical divertor geometry and plasma configuration are key parameters in confining neutrals within the divertor. In particular, vertical target (VT) configurations are considered to better confine neutrals than horizontal configurations as recycling neutrals are preferentially released in the direction of the separatrix and private flux region [1].

In this contribution the effect of the divertor plasma configuration and proximity of the low-field side (LFS) strike point with respect to the LFS pumping plenum is studied for JET ohmically-only heated plasmas in attached and detached divertor conditions. (A complementary study in high-triangularity plasmas is presented in [3].) Key scrape-off layer (SOL) parameters, such as the total ion currents to the plate, I_{div} , and subdivertor pressure, $p_{sub-div}$, for three different divertor plasma configurations are compared, and simulated using the EDGE2D/EIRENE code [4],[5]. Besides a VT configuration, two other configurations were investigated in which the LFS strike point connected to the centre of the load-bearing horizontal tile at the LFS (**V5-stack C**) and one stack radially outboard (**V5/D**) (Fig.1). In all three configurations the high-field side (HFS) strike point was on the HFS vertical target plate. The presented results were obtained during the first campaign in the JET ITER-Like Wall (ILW) materials configuration with a tungsten divertor and a beryllium main chamber. The magnetic shapes in the main chamber were almost identical, including the gaps to main chamber surfaces. Plasmas with low upper-triangularity, δ_u , of approximately 0.2 were chosen. The plasma currents, I_p , and toroidal fields, B_T , were 2.0MA and 2.0T, resulting in an edge safety factor, q_{95} , of 3.4. The plasmas were continuously fuelled with deuterium from top of the vacuum vessel, and in V5/D and VT from both the top and the divertor private flux regions at the highest densities to reach the density limit. The divertor cryo pump, located in the subdivertor at the LFS, was at liquid nitrogen, thus pumping deuterium. The divertor strike point positions were kept constant during the fuelling scan. With increasing fuelling rates, Φ_D , the line-averaged density in the edge of the core plasma, $\langle n_e \rangle_{l,edge}$, also increased (Fig.2a). The latter parameter is used as a proxy for the more difficult to determine upstream separatrix density.

2. MEASUREMENTS

The ohmic heating power, P_{ohm} , and radiated power in the SOL, $P_{rad,SOL}$, were nearly identical for all three divertor plasma configurations, and both parameters increased approximately linearly with increasing $\langle n_e \rangle_{l,edge}$ (Fig.2b). Roughly 3 to 4 times higher fuelling rates were required in VT to obtain the same $\langle n_e \rangle_{l,edge}$ as in V5/C. The density limit was observed to be lowest for V5/C and

highest for VT (approx. 30% higher). The fraction of $P_{\text{rad,SOL}}$ (dominated by deuterium radiation [6]) to P_{ohm} was about 20% at the lowest $\langle n_e \rangle_{1,\text{edge}}$, and saturated at 50% for $\langle n_e \rangle_{1,\text{edge}}$ higher than those at the saturation of $I_{\text{div,LFS}}$.

With increasing $\langle n_e \rangle_{1,\text{edge}}$, $I_{\text{div,LFS}}$ initially increased, saturated at intermediate $\langle n_e \rangle_{1,\text{edge}}$, and then decreased until the density limit was reached (Fig.2c). The divertor plasma configuration had remarkably little effect on both the magnitude of $I_{\text{div,LFS}}$, and $\langle n_e \rangle_{1,\text{edge}}$, at which $I_{\text{div,LFS}}$ saturated: saturation in V5/C occurred at about 10% lower $\langle n_e \rangle_{1,\text{edge}}$ than in VT. The difference in I_{div} between the HFS (not shown) and LFS at their saturation point was also small: $I_{\text{div,HFS}}$ saturated at 5% lower $\langle n_e \rangle_{1,\text{edge}}$ than $I_{\text{div,LFS}}$ in VT, at 10% lower $\langle n_e \rangle_{1,\text{edge}}$ in V5/C and 15% in V5/D.

The neutral pressure in the subdivertor, $p_{\text{sub-div}}$ (Fig. 2d), as well as the Balmer- α emission, D_α , spatially integrated across the LFS divertor leg (not shown) monotonically increased with $\langle n_e \rangle_{1,\text{edge}}$ until the density limit was reached. Both quantities are directly proportional to the neutral density in the divertor, $n_{0,\text{div}}$. The highest $n_{0,\text{div}}$ and particle throughput were observed in VT, which, in turn, explains the need for stronger gas fuelling to reach the same $\langle n_e \rangle_{1,\text{edge}}$. Stronger neutral compression and closer proximity of the LFS strike point to the LFS pumping plenum can explain the about 3 times higher $p_{\text{sub-div}}$ in V5/D than in V5/C.

3. SIMULATIONS

The fluid edge code EDGE2D [4], iteratively coupled to the neutral Monte Carlo code EIRENE [5] was used to simulate the neutral dynamics in the divertor. To fully account ion-neutral interaction and molecular ions at high divertor densities, the currently most complete EIRENE model [7] was used. The measured radial profiles of electron temperature and density at the LFS midplane are used to determine the radial transport coefficients (diffusion only). The code solves the fluid Bragiinski equations in the parallel- \mathbf{B} direction, including the conditions at the divertor plates. Beryllium is the only impurity assumed in the calculations. Cross-field drifts were not invoked; hence, this analysis focuses on the LFS divertor plate only.

The simulations indicate that $I_{\text{div,LFS}}$ saturates at almost the electron density at separatrix at the LFS midplane, $n_{e,\text{sep,LFS-mp}}$, in all three configurations. Unlike the experiments, however, the density limit is reached at lower $n_{e,\text{sep,LFS-mp}}$ in VT (Fig.3a). Despite using the most elaborate EIRENE model, the simulations indicate a 20% reduction of $I_{\text{div,LFS}}$ at the density limit compared to $I_{\text{div,LFS}}$ at its saturation point only (experiment $\sim 3x$). On the other hand, neutrals are predicted to be better confined in VT, leading to, for a given $n_{e,\text{sep,LFS-mp}}$, (i) lower peak temperatures at the LFS target (Fig.3c), (ii) lower neutral currents crossing the separatrix (Fig.3d), and (iii) subsequently lower CX losses in the core (Fig.3f). The peak neutral densities, $n_{0,\text{peak}}$, in the LFS divertor leg are similar; typically $n_{0,\text{peak}}$ peaks at the LFS plate. However, the simulations do not reproduce the experimental finding of the highest pumping in VT (Fig.3b). Hence, other physics processes, such as cross-field drifts and flows from the LFS midplane to the HFS divertor, both potentially leading to a more adequate description of the HFS divertor leg, and divertor bypasses must play an important role

in determining the particle throughput and pumping capability. Assuming that the same physics picture also applies in high confinement plasmas, these results can explain the (a) a lower tungsten content in the plasma (due to lower T_e at the LFS plate) and (b) higher edge temperatures (lower CX losses) in VT configurations (see also [8]).

ACKNOWLEDGEMENTS

This work was supported by EURATOM and carried out within the framework of the European Fusion Development Agreement. The views and opinions expressed herein do not necessarily reflect those of the European Commission.

REFERENCES

- [1]. A. Loarte, et al., *Plasma Physics and Controlled Fusion*, **43** (2011) R183.
- [2]. R.J. Groebner, et al., *Nuclear Fusion* **44** (2004) 204.
- [3]. B. Viola, et al., *this conference*, P1.114.
- [4]. R. Simonini, et al., *Contribution to Plasma Physics* **34** (1994) 368.
- [5]. S. Wiesen, JET ITC-Report, http://www.eirene.de/e2deir_report_30jun06.pdf (2006).
- [6]. K.D. Lawson, et al., *this conference*, P1.101.
- [7]. V. Kotov, et al., *Plasma Physics and Controlled Fusion* **50** (2008) 105012.
- [8]. A. Järvinen, et al., *this conference*, P2.130.

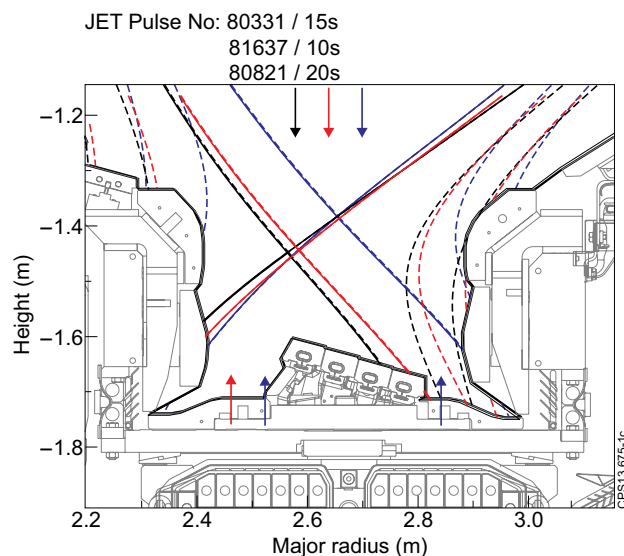


Figure 1: Separatrix and 2cm flux surface (LFS midplane equivalent) for the V5/C (black), V5/D (red) and VT (blue) configurations.

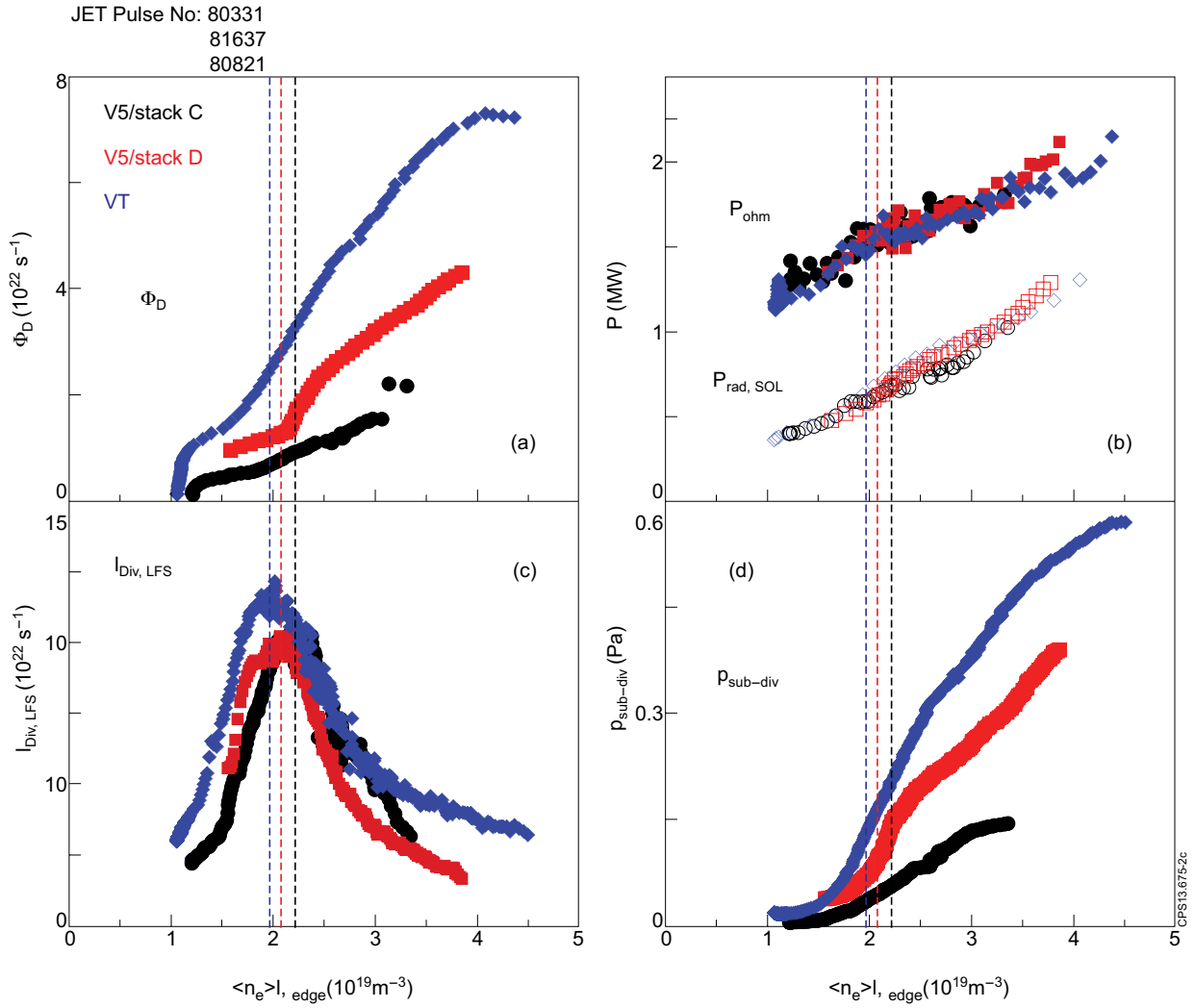


Figure 2: (a) Deuterium gas fuelling, (b) ohmic (solid symbols) and radiated power in the SOL (open), (c) total ion current to the LFS divertor plate, and (d) neutral pressure in the LFS subdivertor as function of $\langle n_e \rangle_{l, \text{edge}}$. The vertical lines indicate $\langle n_e \rangle_{l, \text{edge}}$ at which $I_{\text{div, LFS}}$ saturated.

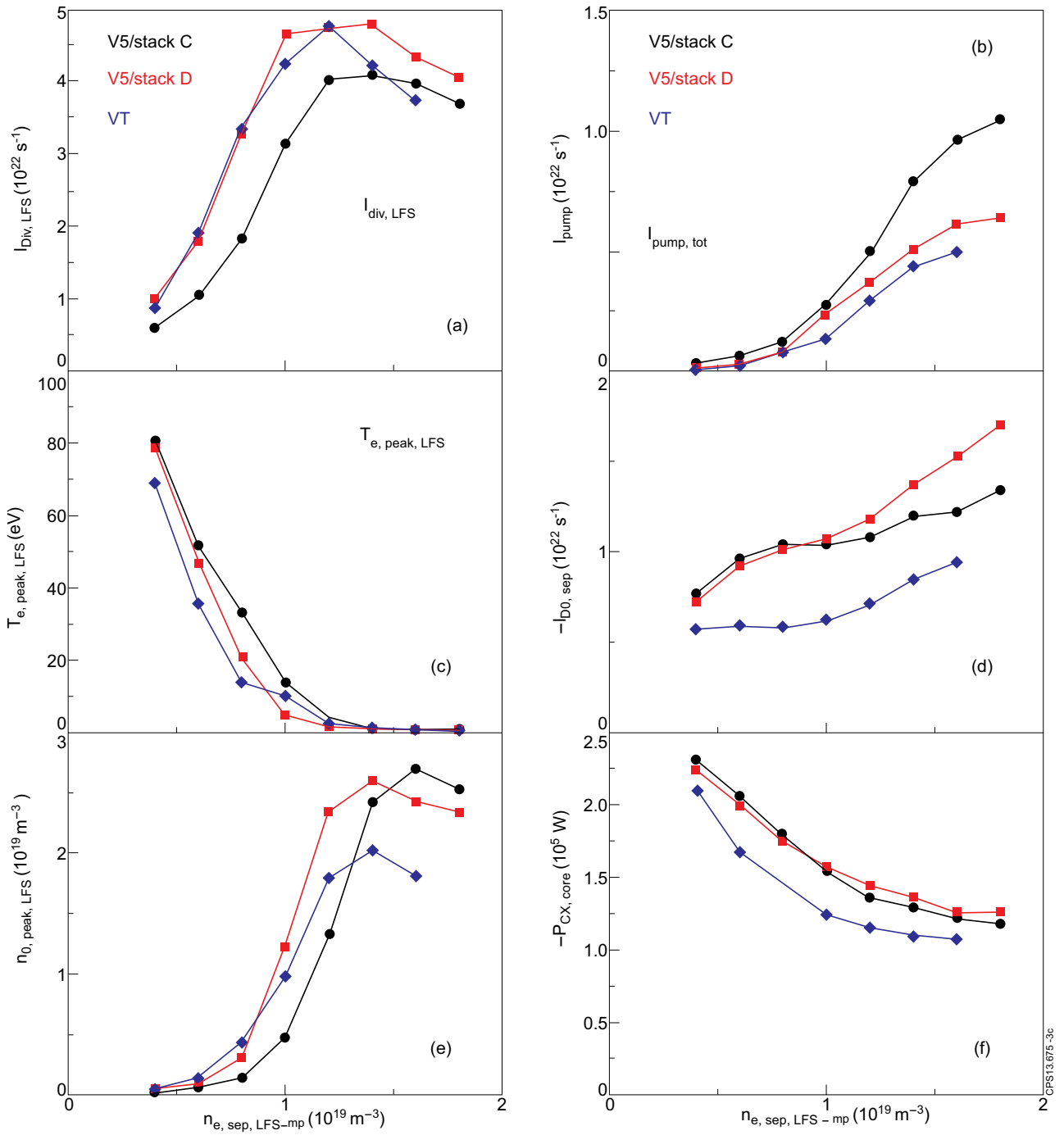


Figure 3: (a) $I_{div,LFS}$, (b) total pumped deuterium, $I_{pump,tot}$, (c) $T_{e,peak,LFS-plate}$, (d) total atomic deuterium current total ion current across separatrix, (e) peak neutral deuterium density in the LFS divertor leg, and (f) charge exchange loss power in the core as function of $n_{e,sep,LFS-mp}$.